"A Cochlear Nucleus Auditory

Prosthesis based on microstimulation”

Contract No. **No. NO1-DC-4-0005**
Progress Report #10

HUNTINGTON MEDICAL RESEARCH INSTITUTES
NEURAL ENGINEERING LABORATORY
734 Fairmount Avenue
Pasadena, California 91105

D.B. McCreery, PhD

HOUSE EAR INSTITUTE
2100 WEST THIRD STREET
Los Angeles, California 90057

R.V. Shannon, PhD
Steve Otto, MS

SUMMARY AND ABSTRACT

I: Activities at Huntington Medical Research Institutes

Part of the work scope this project is to objectively compare the ability of penetrating microstimulating electrodes and surface macroelectrodes to selective access the tonotopic organization of the ventral cochlear nucleus. We have begun these studies using a modified version of our microstimulating cochlear nucleus arrays, with 16 microstimulating sites on 4-shanks, and with 2 surface macroelectrodes (geometric area of approximately 0.4 $mm^{2)}$ on the under surface of the array superstructure. Data sets were obtained from 2 cats. Multiunit neuronal activity was recorded at 16 sites along the tonotopic gradient of the central nucleus of the contralateral inferior colliculus (ICC), while stimulating in the contralateral ventral cochlear nucleus with either the surface electrodes or the intranuclear microelectrodes. The spectral selectivity of the surface electrodes and penetrating microelectrodes was quantified according to the relation between the amount of induced neuronal activity and the distribution of the activity along the tonotopic gradient of the ICC. Two measures of dispersion of neuronal activity were used (dispersion of activity close to the activity centroid, and dispersion of activity recorded over most of the recording array) and two measures of the magnitude of neuronal activity (also based on activity close to the centroid, and activity recorded over much of the recording array). By all measures, the neural activity induced by the penetrating microstimulating electrodes was more restricted along the tonotopic gradient of most of the ICC than was the activity from the small surface electrodes. That is, the penetrating microelectrodes displayed greater spectral specificity. However, the results from one animal (penetration 3 from CN162) indicate that, in the most rostral part of the ICC, the spectral specificity is comparable for both types of electrodes. This will be examined further in subsequent animals, during the next quarter.

II Activities at the House Ear institute

To date, auditory brainstem implants each with an array of surface electrodes and an array of 8 or 10 penetrating microstimulating electrodes ("PABI configuration) have been implanted into nine patients with Type 2 Neurofibromatosis. PABI patients 4, 6, 7, 8 and 9 were tested in this quarter. Patients 8 and 9 were seen for initial stimulation and 4, 6, and 7 were seen during their routine follow-up visits.

Measures on PABI patients in this quarter showed a mixed picture of results. In the two new PABI patients tested in this quarter only one had useful auditory sensations on the penetrating electrodes, and she only had one usable penetrating electrode. In total, four of 9 PABI patients receive no auditory sensations on the penetrating electrodes and three of the other five only receive auditory sensations on one penetrating electrode. We continue to observe speech recognition performance in PABI patients that is similar to that of surface ABI patients. We see little improvement in speech recognition performance out to three years. Psychophysical measures show some PABI patients to perform significantly worse than surface ABI and CI patients, while most are similar to ABI and CI listeners. The only psychophysical measure that is different in some PABI patients is the integration of pulses as a function of pulse rate, resulting in lower thresholds as rate increases. The cause of this difference is not clear at this time and this difference does not appear to be related to speech recognition performance.

I: Work at Huntington Medical Research Institutes

Comparisons of spectral specificity of micro-and macrostimulating electrodes in the cat cochlear nucleus.

Part of the work scope of our contract call for us to objectively compare the ability of penetrating microstimulating electrodes and surface macroelectrodes to selective access the tonotopic organization of the ventral cochlear nucleus. We have begun these studies using a modified version of the microstimulating arrays with 16 stimulating sites on 4-shanks, and with 2 macroelectrodes on the under surface. Figure 1A shows a multisite silicon substrate probe with 2 shanks and 8 stimulating sites sputter-coated with iridium oxide. The probes were fabricated at the University of Michigan under the direction of Design Engineer Jamille Hetke, and provided to us through NeuroNexus, Inc. The 4 electrode sites on each shank are 0.8 to 1.7 mm below the probe's transverse spine. After bonding of the Parylene-coated gold lead wires, the transverse spines of two probes were encapsulated in EpoTek 301 epoxy to form the button superstructure, 2.5 mm in diameter. The 8 or 16 lead wires were wound into a helical cable and encapsulated in silicone elastomer. A complete array of 2 probes (4 shanks and 16 electrode sites) extending from the epoxy superstructure is shown in figure 1B.

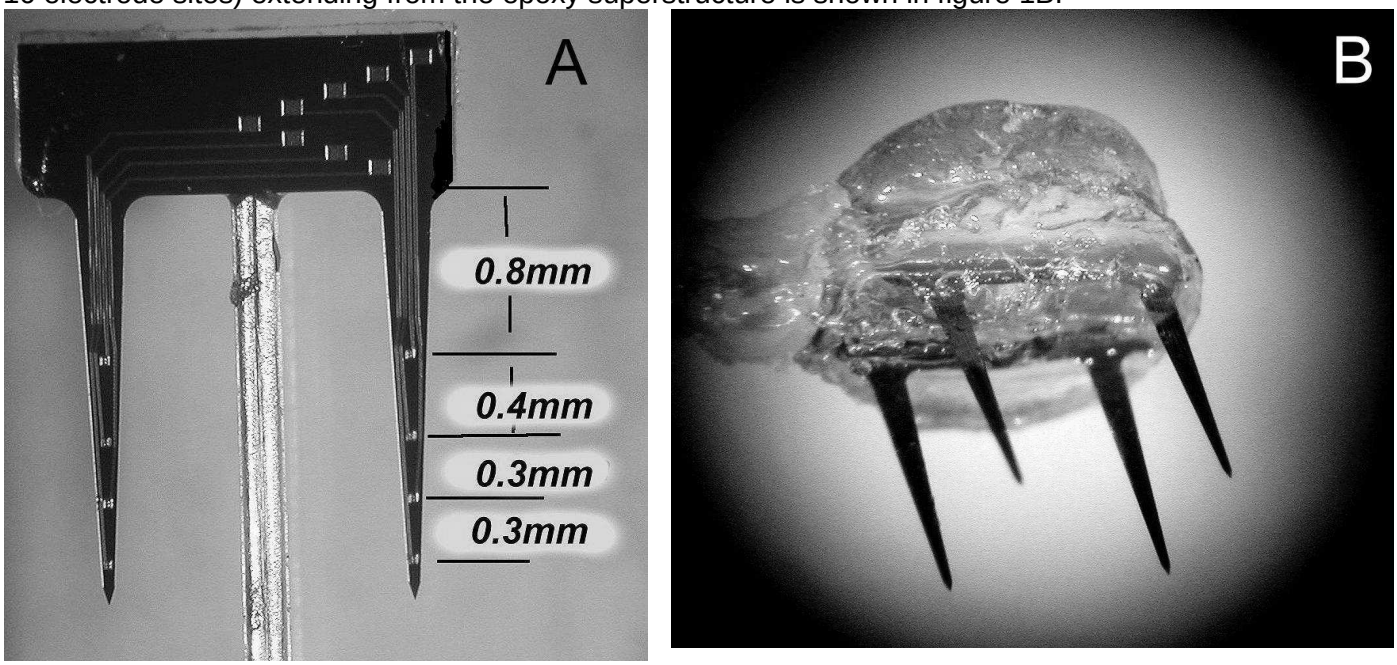

Figure 1

The rectangular platinum macroelectrodes have a geometric area of approximately 0.4 mm^2, as in the surface array now used in the auditory brainstem implant (ABI) program. These and are set between the silicon shanks, which in figure 2 are oriented towards the camera. The array superstructure is implanted on the dorsolateral surface of the cochlear nucleus, with one macroelectrode dorsal and medial and the second ventral and lateral, so that the medial macroelectrode will have a chance to access the high acoustic frequencies and the lateral electrode will access low frequencies. The silicon

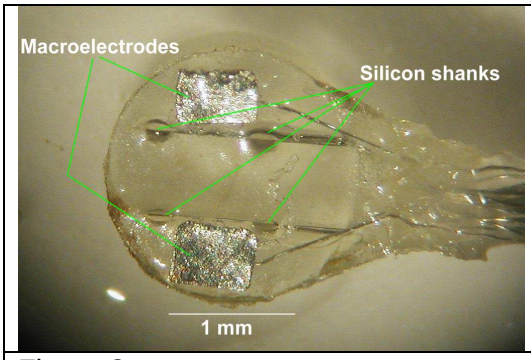

Figure 2

shanks penetrate into the ventral cochlear nucleus. In our cat model, the spread of neuronal activity along the tonotopic gradient of the ventral cochlear nucleus is quantified as the spread of activity along the dorsolateral-ventromedial axis of the central nucleus of the inferior colliculus, using the methods described in our pervious quarterly reports, and summarized below.

These were acute experiments. The cats were anesthetized with Isoflurane and oxygen, and their heads fixed in a stereotaxic frame. To facilitate delivery of acoustic stimuli, a hollow earbar was used contralateral to the inferior colliculus from which recordings were made. The ipsilateral earbar was solid, in order to attenuate acoustic stimuli. A craniectomy was made over the cerebellum on the right side and part of the lateral cerebellum was aspirated. The array of stimulating microelectrodes was secured against the orifice of a vacuum wand, and advanced into the CN at approximately 45^{o} from the vertical; approximately the angle at which a microelectrode array would be inserted into the human CN, using the translabyrinthine approach to brainstem. The array cable was fixed to the bone at the margin of the craniectomy and the cavity was filled with gelfoam. A wide craniectomy was made over the left cerebral hemisphere, and the occipital pole of the cerebrum was removed to expose the dorsal surface of the inferior colliculus. The cat was transferred to a double-wall sound isolation booth (Audiometrics 120A-SP).Throughout the experiment, respiration rate and end-tidal CO_2 were monitored continuously. Core body temperature was maintained at 37-39℃. All sound-generating equipment was outside of the sound isolation room.

The tonotopic organization of the anteroventral and posteroventral CN is preserved in the projection from the CN to the ICC, where the iso-frequency laminae are oriented approximately perpendicular to its dorsolateral-ventromedial (DLVM) axis, with low acoustic frequencies represented dorsally and laterally and high frequencies represented ventrally and medially. Multiunit neuronal activity was recorded at 16 locations separated by 200 μm and spanning 3 mm along the DLVM axis of ICC, using a multisite probe fabricated by NeuroNexus, Inc. For each insertion of the recording probe, tone bursts ranging from 0.5 to 25 kHz, and 100 ms in duration with a rise time of 10 ms, were delivered through a broad-band loudspeaker (~ ±5 db, 200 Hz to 35 kHz). When a large, well-isolated extracellular action potential was recorded at one of the sites in the ICC, its best frequency near threshold (BF) was determined by successive small adjustments of the acoustic frequency and reductions in the stimulus intensity.

After the acoustic mapping, 1500 controlled-current, biphasic stimulus pulses (150 μs/ph in duration at 50 pps) were applied to each of the microelectrode sites in the CN. The stimulus current was 10, 20 or 30 μA (1.5, 3 or 4.5 nC/phase). In the human patients who have been implanted with arrays of single-site iridium microstimulating electrodes in their cochlear nuclei, the thresholds for auditory percepts have been 1 to 2 nC/phase for most of the penetrating microelectrodes .

Extracellular action potentials (multiunit activity, MUA) evoked by the stimulation in the VCN were separated from the large compound response using a common background suppression technique and bandpass filtering between 500 Hz and 8 kHz. Action potentials were sorted into bins 100 μs in width and summed over the 1500 presentation of the stimulus, yielding 16 PST (post-stimulus time) histograms, one for each recording site in the ICC. The 16 histograms represent, in PST and depth in the ICC, the MUA evoked in response to the stimulation in the VCN. Response maps of the MUA (Figure 5) were generated from the 16 PST histograms, and the centroids of the activity were computed as the means, in depth in the ICC and PST, of the counts of the MUA from the bins comprising the maps. Computation of the maps' centroids can be seriously skewed by MUA that is far from the maximum neuronal response to the electrical stimulus in the VCN. This background activity is present in most of the bins of the PST histograms, but it contributes only a few counts to each histogram bin. Thus the centroids were generated only from histograms bins in which the spike count was at least 50% of the "averaged maximum count" (AMC). The histogram's maxima is well defined by the average of the counts in the 4 bins (the 400 ms window) around the peak, so we computed this 4-bin average for each of the 16 histograms and selected the largest of these as the AMC. This procedure also accommodates the fact that the span of the feline ICC is greater than the span of the

recording array. By computing the centroids only from the bins that are fairly close to the 4 bins contributing to the AMC, we also reduce "edge artifact" whereby centroids near the upper or lower extremes of the recording array tend to be computed as being closer to the center of the array than is actually the case .

The spread of neuronal activity around the centroid in the ICC was quantified in two ways .One measure ("Span 50") is the extent of the iso-response (contour) lines corresponding to the range of bin counts between 50% and 100% of the AMC (see Figure 5A) . Since each map is normalized on its own AMC, the computation of the activity span is not affected by the absolute magnitude of the neuronal activity evoked from each site in the VCN. This measure involves only the neuronal activity recorded by the electrodes close to the centroid, and thus is relatively immune to the edge artifact. The second measure ("SD of span") is the square root of the second central moment of the activity around the centroid. This is mathematically identical to the standard deviation about the mean, and thus a commonly-used measure of dispersion of a random variable about its mean. To reduce the influence of background activity on this computation, only bins from the PST histogram in which the activity was at least 10% of the AMC were used. Overall, "sd of span" probably is a more objective metric for this distribution of neuronal activity along the tonotopic gradient of the ICC, but because it includes neuronal activity recorded some distance from the centroid, we expect it to be more vulnerable to edge artifact, especially when the centroid is close to the deepest or shallowest recording sites.

For both penetrating microelectrodes and surface macroelectrodes, the spread of neuronal activity increases somewhat with stimulus amplitude. Thus an objective comparison of the spatial selectivity of the micro and macro electrodes dictates that we compare the relation between the amount of induced neuronal activity and the distribution of the activity along the DLVM axis of the ICC. One measure of neuronal activity, designated "maximum activity" is the averaged maximum count (AMC) as defined above. However, AMC is computed from the activity of only a few neurons in one PST histogram near the centroid, and the dynamic range of loudness percepts far exceeds the dynamic range of individual neurons in the ICC (Ehret and M. M. Merzenich, 1988, Dean et al, 2005). Human patients with auditory brainstem report that loudness increases monotonically with stimulus amplitude, for both surface and penetrating electrodes. In cats, the compound action potential recorded from the rostral pole of the inferior colliculus also increases with stimulus amplitude (McCreery et al, 1997, 2000, 2007). This growth with stimulus amplitude presumably reflects the recruitment of more neurons, more activity from individual neurons and closer temporal synchrony of the induced neuronal activity. Thus our second measure of neuronal activity, "total spikes" is the total neuronal activity in all bins of all 16 PST histograms for all 1500 data acquisitions at a given stimulus amplitude. It also increases with stimulus amplitude, for the surface and penetrating electrodes, although the surface electrodes require more current to induce a comparable amount of neuronal activity, as shown in Figure 3, from cat CN163.

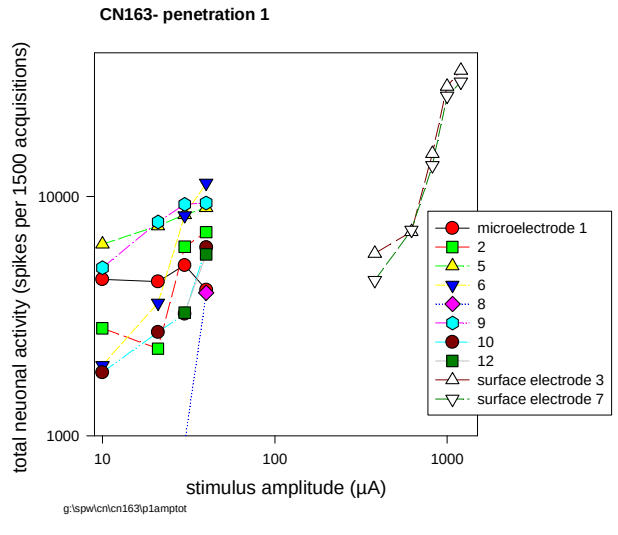

Figure 3

RESULTS

Data were obtained from 2 cats (CN162 and CN163). The diagram in the left panel of Figure 4 shows the locations of the microstimulating sites on 3 of the shanks of the microelectrode array that was used in both animals and also the locations of the 2 surface electrodes on the underside of the epoxy superstructure. The microelectrode sites on the rostrolateral shank were not functional, and 2 of these channels (3 and 7) were used for the surface electrodes. Microelectrode channels 1, 4, 5, 8, 9, 10, 13 and 16 were in the caudal posteroventral cochlear nucleus, and sites 2, 6, 10 and 14 were in the rostral PVCN. The 2 right panels of Figure 4 depict the points on the surface of the contralateral IC at which the recording

array penetrated into the nucleus; the recording array then penetrated into the IC and down into the ICC at an angle of approximately 45°from the verti cal.

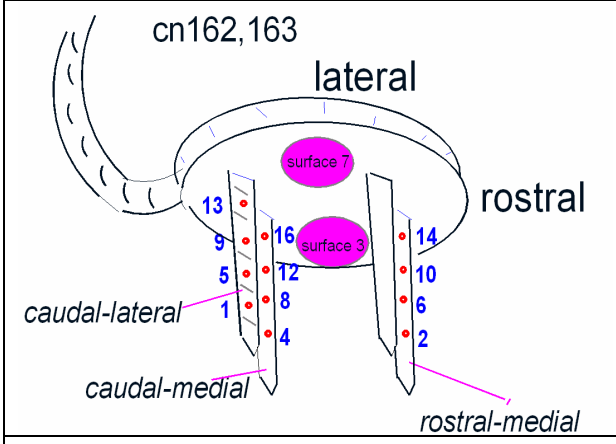

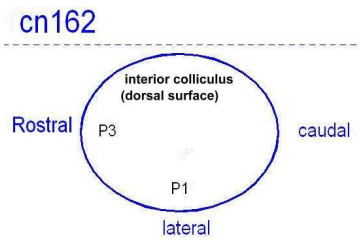

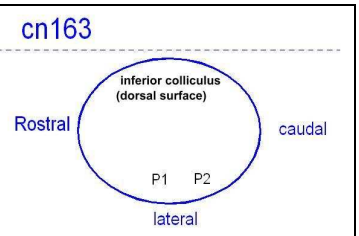

Figure 4

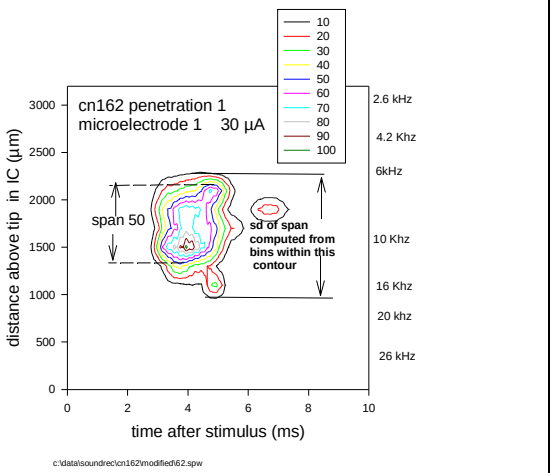

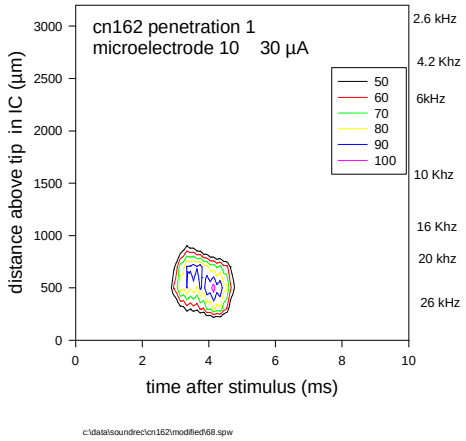

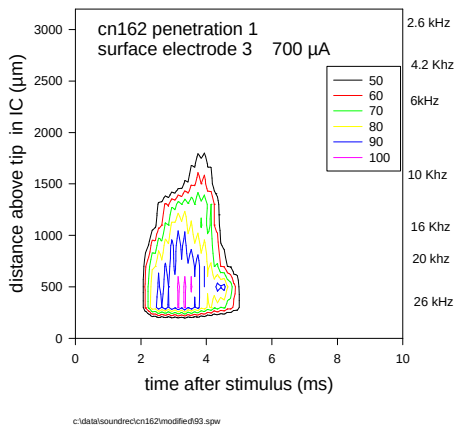

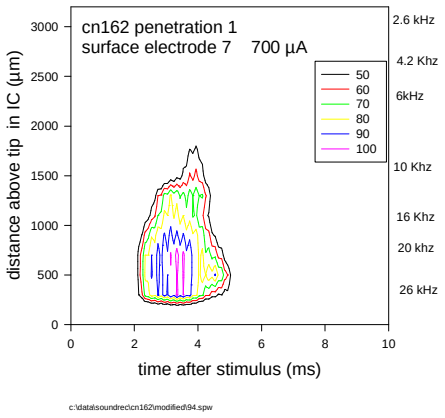

Figure 5

Figure 5 shows contour maps of the responses during penetration 1 into the lateral ICC of cat CN162 while stimulating in the contralateral ventral cochlear nucleus at 30 µA with microelectrodes 1 or 10, and at 700 µA with either of the 2 surface electrodes (electrodes 3 and 7). The abscissa is time after onset of the stimulus pulse. The left ordinate is the distance above the deepest recording site along the DLVM axis of ICC. The corresponding acoustic map is shown on the right ordinate. The

maps are normalized on 100% of the averaged maximum spike count (AMC), in gradations of 10% of the AMC. The upper left panel illustrates how the two measures of dispersion, "Span 50" and "SD of span" are calculated. The other panels show only the contour lines between 50% and 100% of the AMC. The maximum response is 3.5-4 ms after onset of the stimulus, for both the surface electrodes and the penetrating microelectrodes.

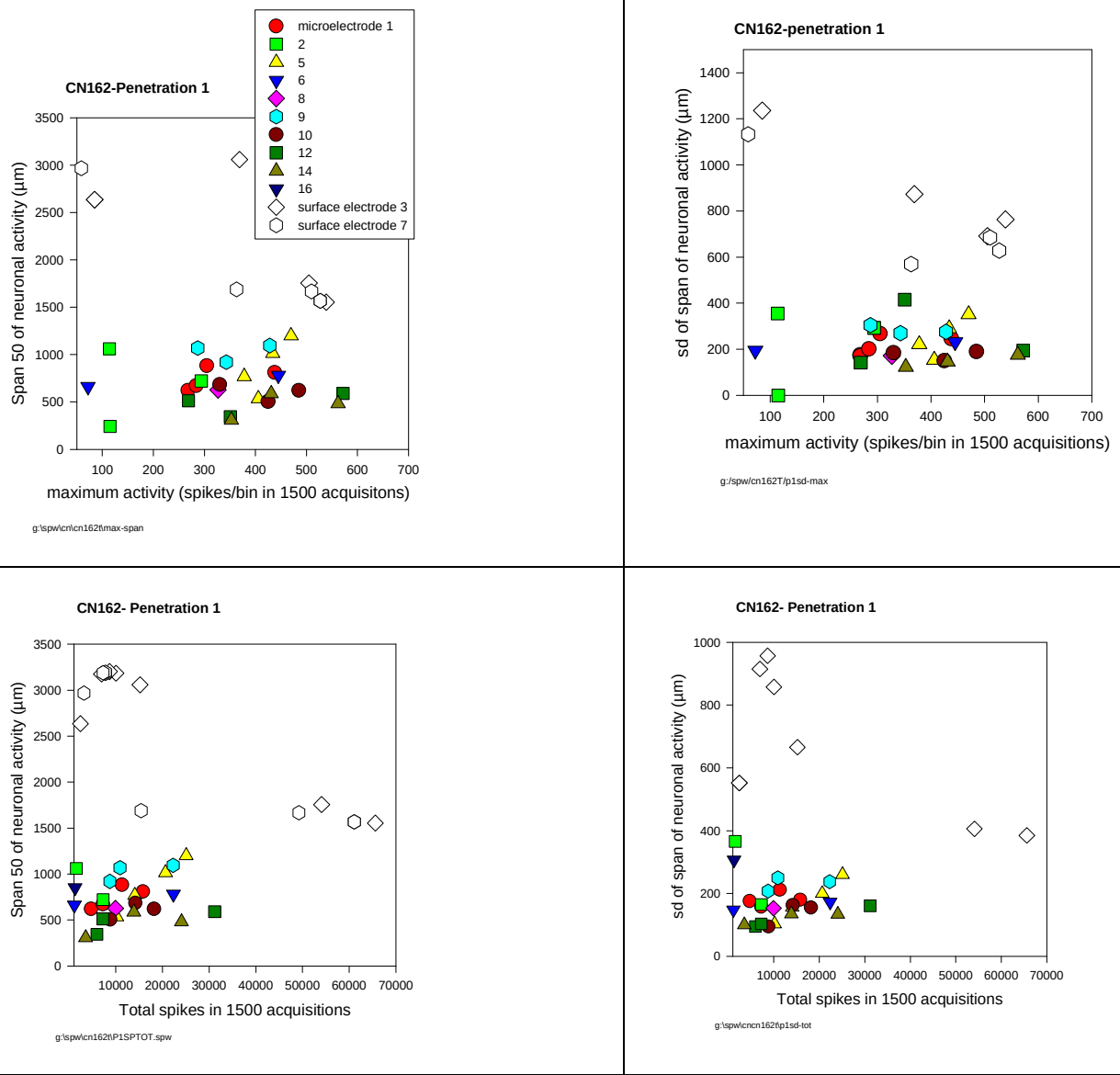

Figure 6

Figure 6 shows the "span 50" (left panels) and "SD of span" (right panels) plotted against the AMC (top panels) and the total spikes in all bins of all of the PST histograms (lower panels). Data are shown for 10 microelectrodes from which responses could be recorded at 40 µA or less and for the 2 surface electrodes. Each microelectrode or surface electrode is represented by multiple data points corresponding to the responses to different stimulus amplitudes, between 10 and 40 µA for the penetrating microelectrodes, and 500-1200 µA for the surface electrodes. Only those data points were used for the stimulus in the CN induced sufficient neuronal activity so that the depth of the centroid did not change by more than 100 µm over two successive levels of stimulus amplitude. By all measures, the microelectrodes produced less spread of neuronal activity along the DLVM axis of the ICC than did the surface electrodes. Interestingly, the span of the activity from the surface electrodes was less when the stimulus amplitude was very high and the total activity was correspondingly large (and greater than what could be evoked by the penetrating microelectrodes). However, across the full range of responses, the Span 50 and sd of the span was greater for the surface electrodes.

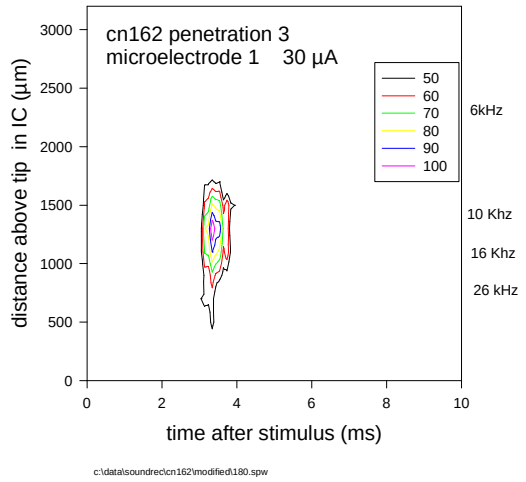

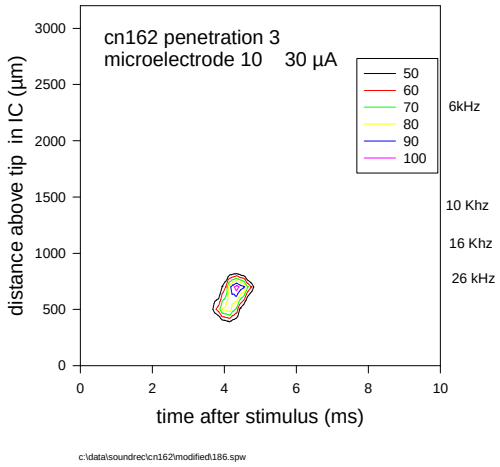

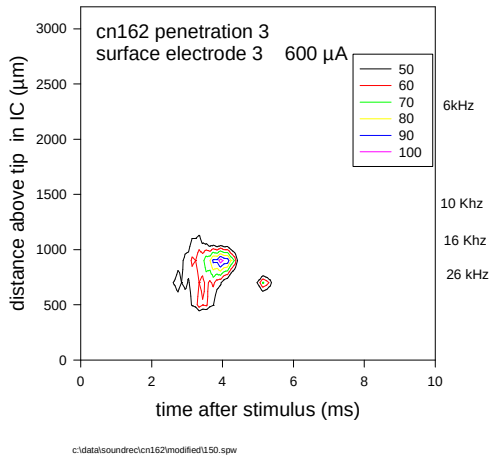

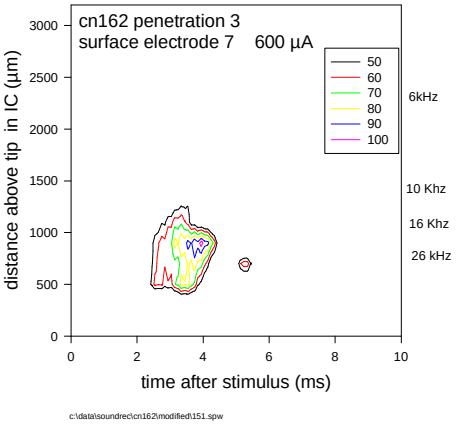

Figure 7

Figure 7 shows the contour maps of the responses evoked from 2 microelectrodes and 2 surface electrodes during penetration 3 into the rostral pole of the ICC of cat CN162 (See Figure 4)

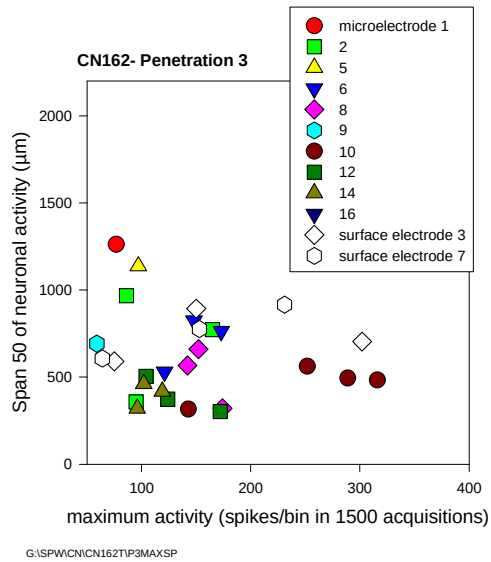

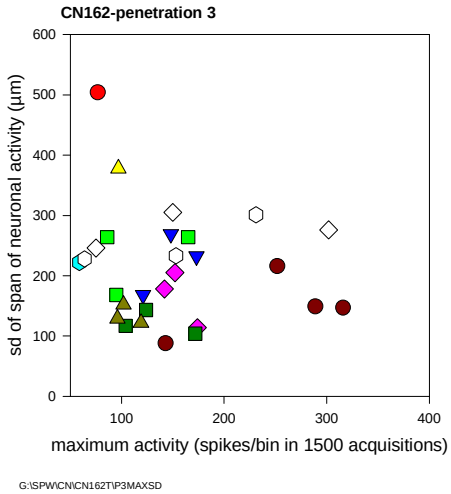

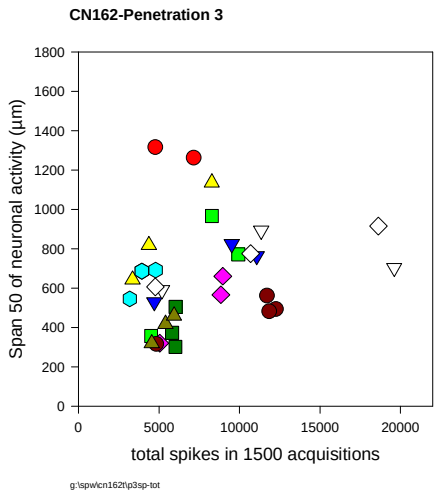

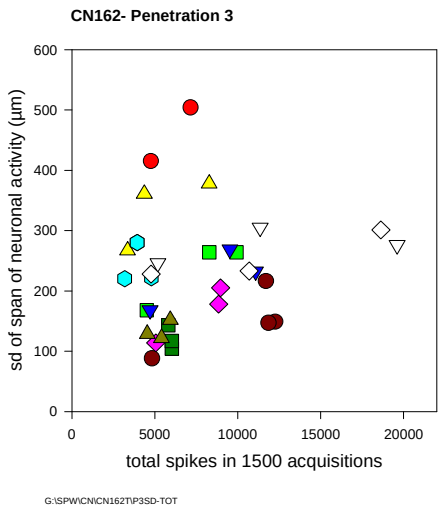

Figure 8

Figure 8 shows the activity- response relations for penetration 3. The stimulation in the ventral CN produced less activity in this part of the ICC, although the stimulating array had not moved (compare Figures 6 and 8), but over a corresponding range of AMC and total spikes, the span of the activity from the surface electrodes was less than for penetration 1, and was comparable to that of the penetrating microelectrodes. Only the shallow microelectrodes in the high-frequency region of the ventral cochlear nucleus produced less spread of activity than did the surface electrodes. The surface electrodes rest directly on the dorsal cochlear nucleus, and it is possible that the small spread of activity in the rostral ICC is due to a projection from a restricted region of the dorsal nucleus. The fusiform and giant cells of the feline dorsal cochlear nucleus project directly to the contralateral ICC (Cant, 2003; Oliver, 1985).

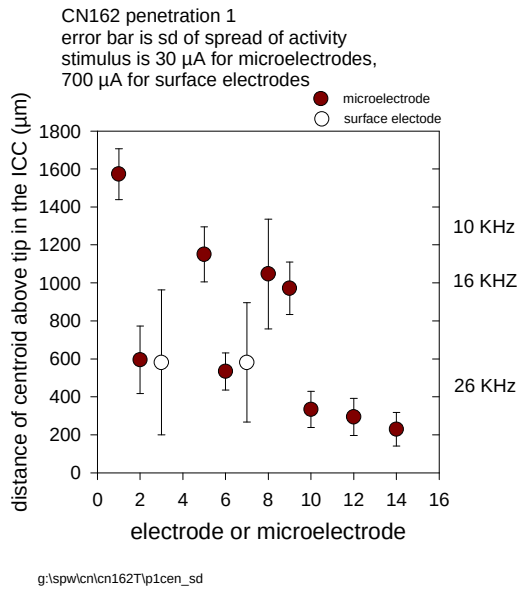

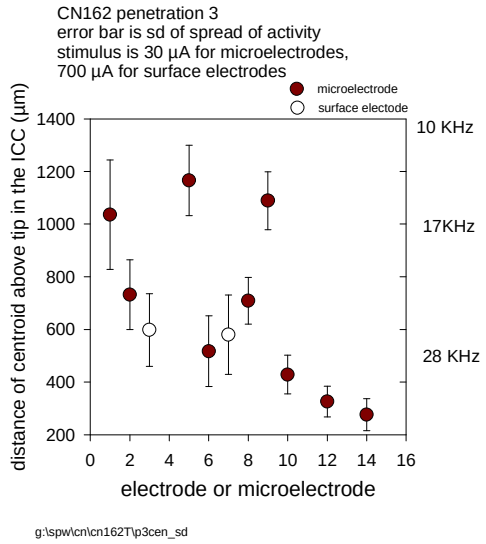

Figure 9

Figure 9 shows the locations of the centroids of the activity in the ICC and the SD of the span of the activity for penetrations 1 and 3 into the ICC of cat CN162. Note that for penetration 3, only the shallow microelectrodes in the high-frequency region of the ventral cochlear nucleus produce less spread of activity than the surface electrodes.

The differences in the responses for penetrations 1 and 3 again illustrate that the isofrequency lamina of the ICC are not homogenous over their mediolateral and rostrocaudal expanses, and should serve as a note of caution for proposals to record from the ICC using chronically-implanted microelectrode arrays. Typically, only the rostral pole of the feline ICC (corresponding approximately to the location of penetration 3) is accessible without resecting the ossified tentorium . Removal of the tentorium is difficult in a survival surgery since access requires either ablation of a substantial part of the posterior cerebrum or a major retraction of the posterior cerebrum. We are presently evaluating an approach by which the entire tentorium is removed on one side by a posterior approach, beginning at the point at which it fused to the calvarium, and working rostrally.

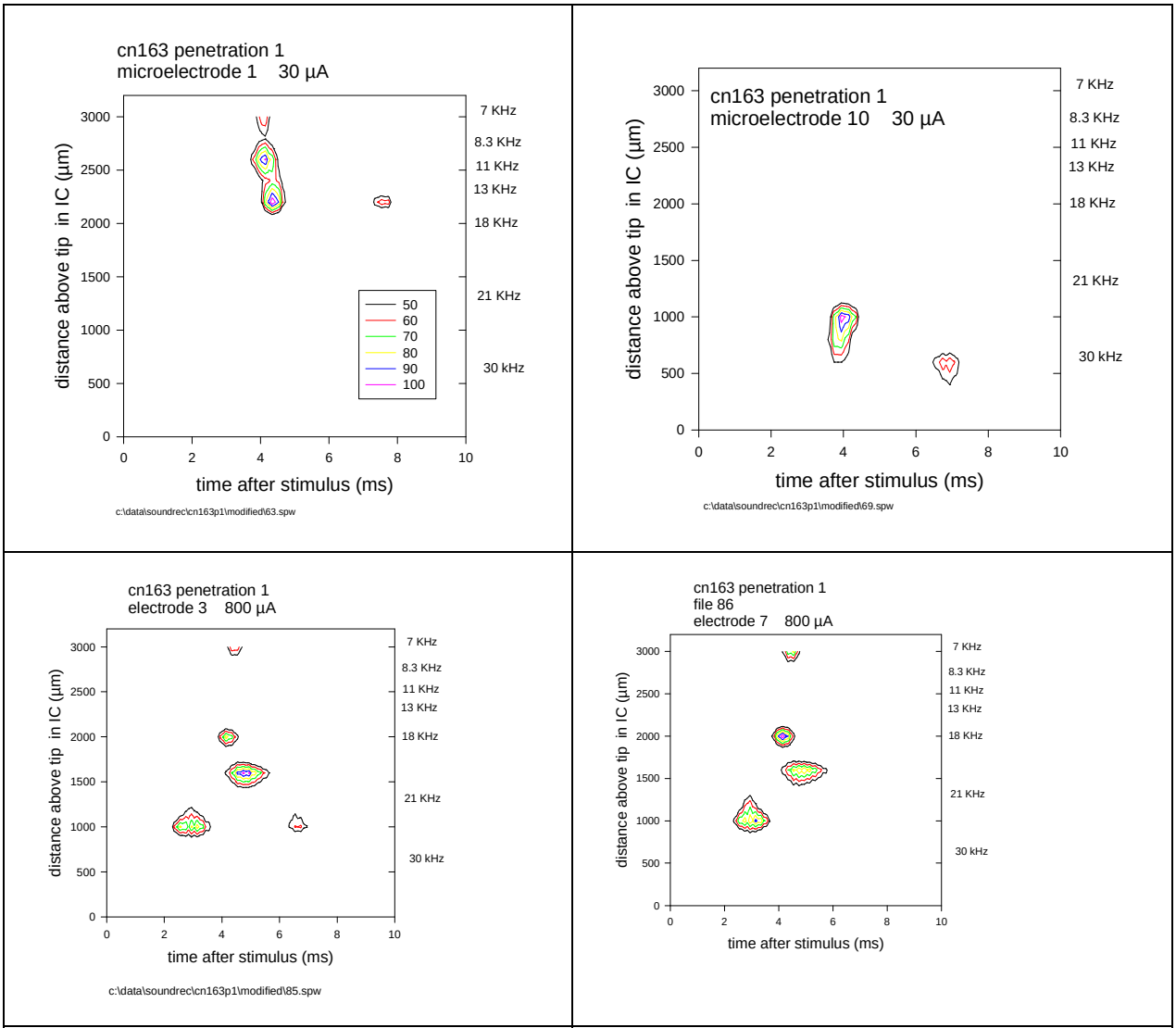

Figure 10

Figure 10 shows the maps of the activity evoked by 2 of the microelectrodes and by the 2 surface electrodes for penetration 1 into the ICC of cat CN163. In this animal, the microelectrode array was somewhat more lateral in the CN than in cat CN162. Penetration 1 into the inferior colliculus was at a location comparable to that of penetration 1 in cat CN162 (see Figure 4). The activity from the microelectrodes and from the surface electrodes spanned a wider range of post-stimulus times than in cat CN162, with the microelectrodes producing more late activity (at about 7 ms after the stimulus) and the surface electrodes producing more early activity, at about 3 ms after the stimulus. This suggests that the surface and penetrating microelectrodes were, at least to some extent, activating different neuronal populations in the cochlear nucleus and different projections into the IC.

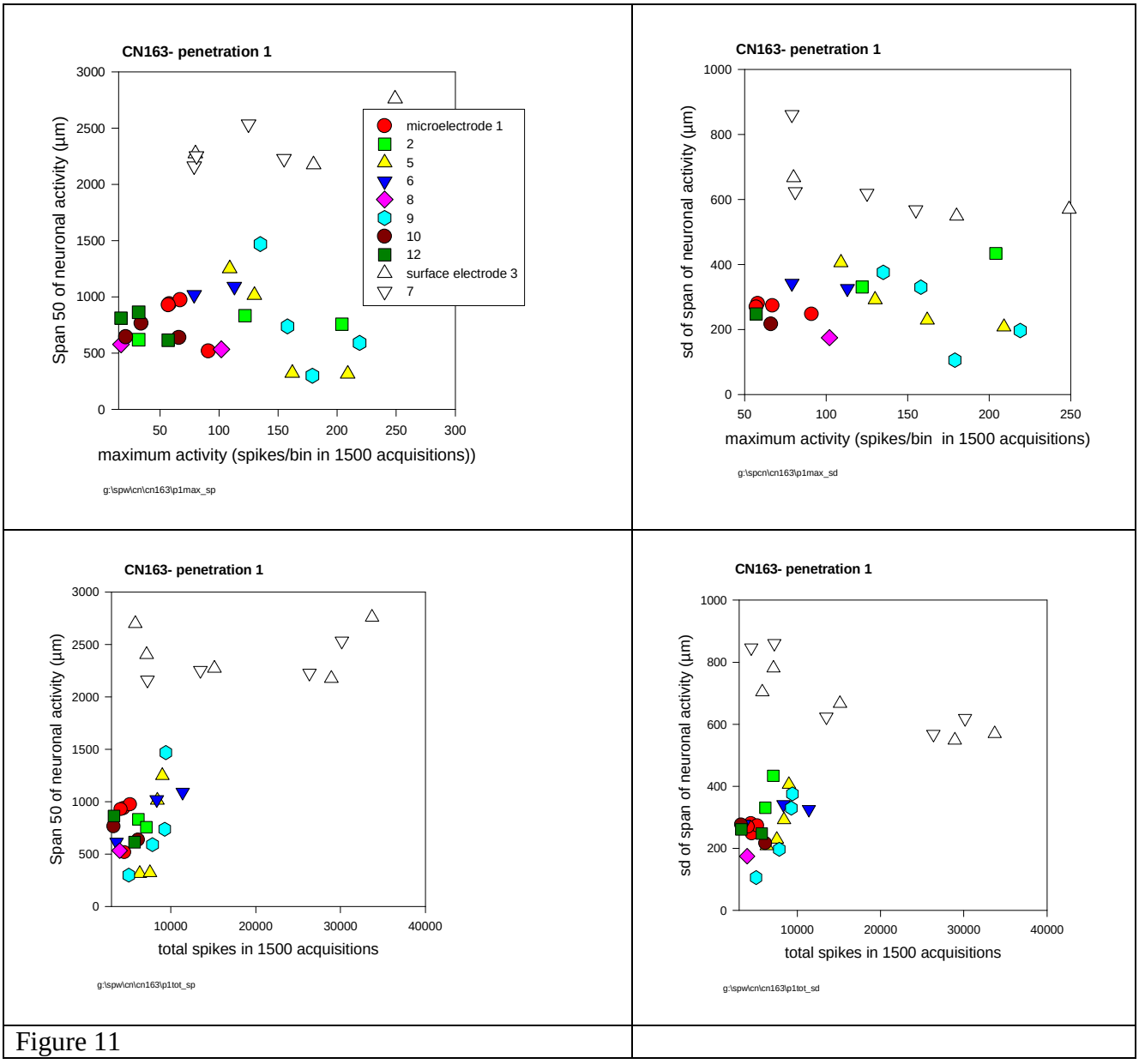

Figure 11

Figures 11 and 12 show plots of neural activity vs. span and sd of the span for penetrations 1 and 2 in cat CN163. Penetration 2 was slightly caudal of penetration 1, but still from the most lateral part of the IC (see Figure 4). For both penetrations, the Span 50 and the sd of the span was greater for the surface electrodes. Figure 13 shows the locations of the centroids of the activity in the ICC and the SD of the spans of the activity for both penetrations.

In conclusion, the results from these two animals indicate that the neural activity induced by the penetrating microstimulating electrodes was more restricted along the tonotopic gradient of most of the ICC than was the activity from the small surface electrodes. That is, the penetrating microelectrodes displayed greater spectral specificity. However, the results from one animal (penetration 3 from CN162) indicate that, in the most rostral part of the ICC, the spectral specificity is comparable for both types of electrodes. This will be examined further in subsequent animals, during the next quarter.

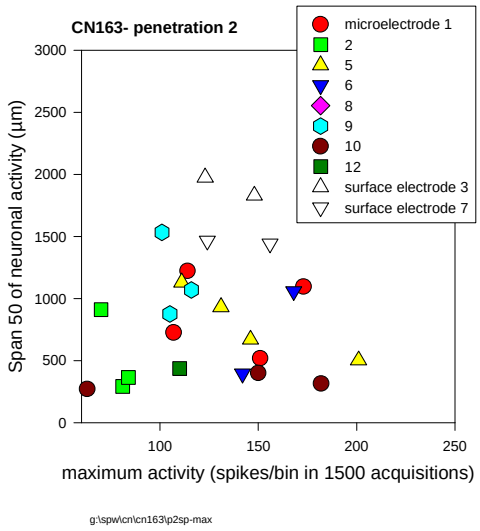
CN163- penetration 2
microelectrode 1
2
5
6
8
9
10
12
surface electrode 3
surface electrode 7
Span 50 of neuronal activity (µm)
maximum activity (spikes/bin in 1500 acquisitions)
g:\spw\cn\cn163\p2sp-max

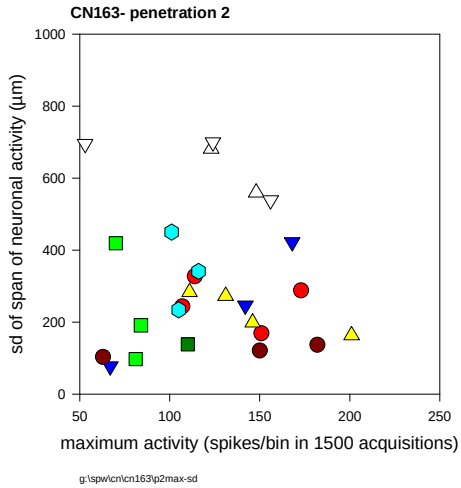
CN163- penetration 2
sd of span of neuronal activity (µm)
maximum activity (spikes/bin in 1500 acquisitions)
g:\spw\cn\cn163\p2max-sd

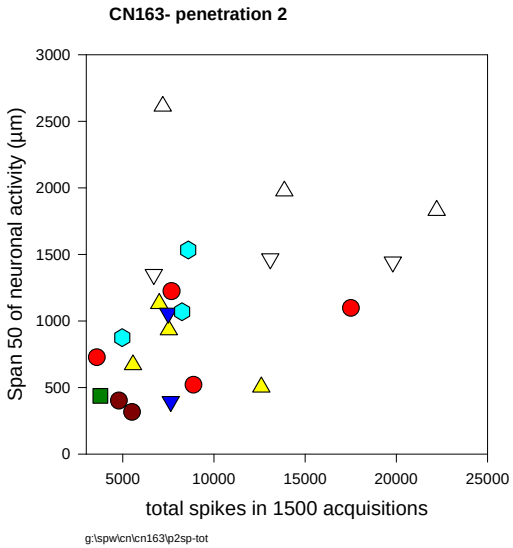
CN163- penetration 2
Span 50 of neuronal activity (µm)
total spikes in 1500 acquisitions
g:\spw\cn\cn163\p2sp-tot

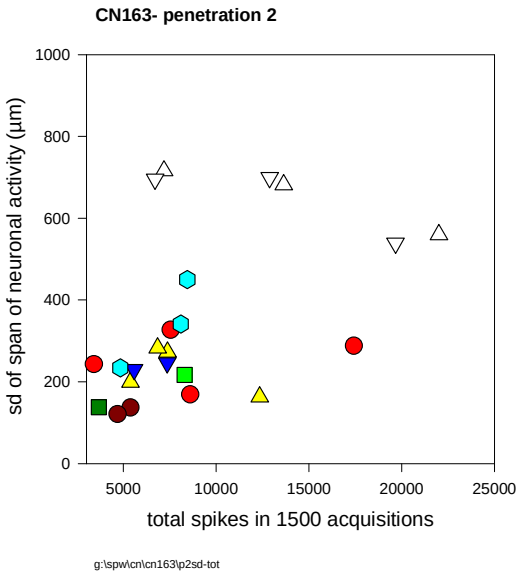
CN163- penetration 2
sd of span of neuronal activity (µm)
total spikes in 1500 acquisitions
g:\spw\cn\cn163\p2sd-tot

Figure 12

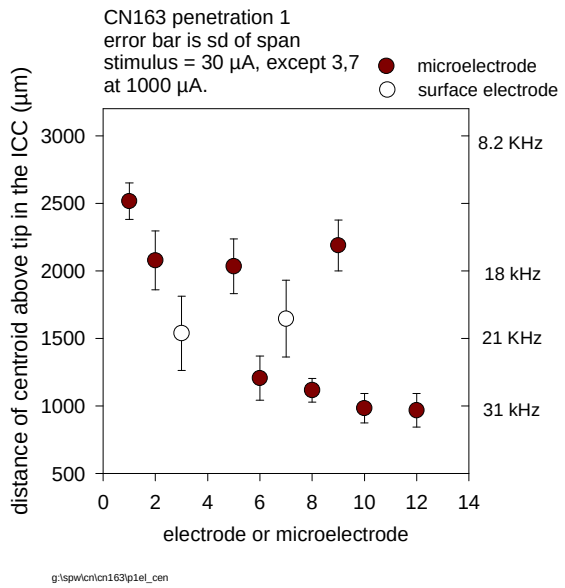

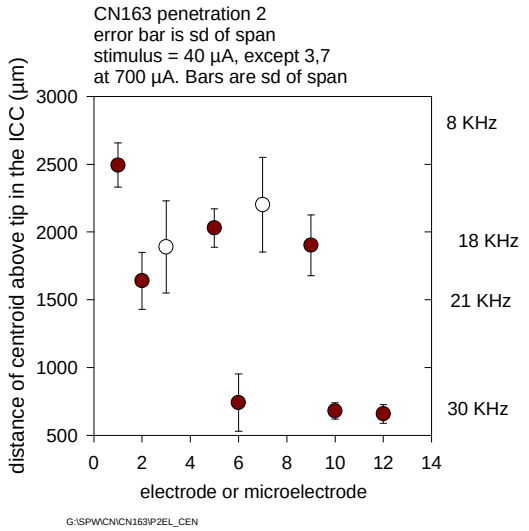

Figure 13

REFERENCES

G. Ehret and M. M. Merzenich, "Neuronal discharge rate is unsuitable for encoding sound intensity at the inferior-colliculus level," *Hear Res*, vol. 35, pp. 1-7, 1988.

Dean, N. S. Harper, and D. McAlpine, "Neural population coding of sound level adapts to stimulus statistics," *Nat Neurosci*, vol. 8, pp. 1684-9, 2005.

D. McCreery, A. Lossinsky, and V. Pikov, "Performance of multisite silicon microprobes implanted chronically in the ventral cochlear nucleus of the cat," *Accepted for publication in IEEE Trans. Biomed. Engr.*, 2007

D. B. McCreery, T. G. Yuen, and L. A. Bullara, "Chronic microstimulation in the feline ventral cochlear nucleus: physiologic and histologic effects," *Hear Res*, vol. 149, pp. 223-38, 2000

D. B. McCreery, T. G. Yuen, W. F. Agnew, and L. A. Bullara, "A characterization of the effects on neuronal excitability due to prolonged microstimulation with chronically implanted microelectrodes," *IEEE Trans Biomed Eng*, vol. 44, pp. 931-9, 1997.

II: Activities at the House Ear Institute

HEI/HMRI PABI Contract
QPR 06d
October-November-December 2006

Overview

To date, auditory brainstem implants each with an array of surface electrodes and an array of 8 or 10 penetrating microstimulating electrodes ("PABI configuration) have been implanted into nine patients with Type 2 Neurofibromatosis. PABI patients 4, 6, 7, 8 and 9 were tested in this quarter. Patients 8 and 9 were seen for initial stimulation and 4, 6, and 7 were seen during their routine follow-up visits.

Threshold and Dynamic Range

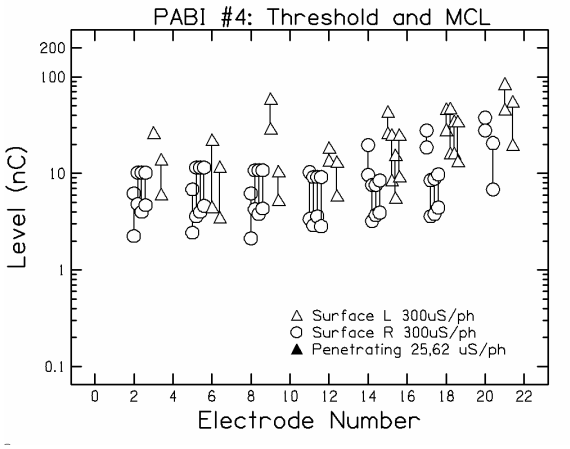

Figure 1

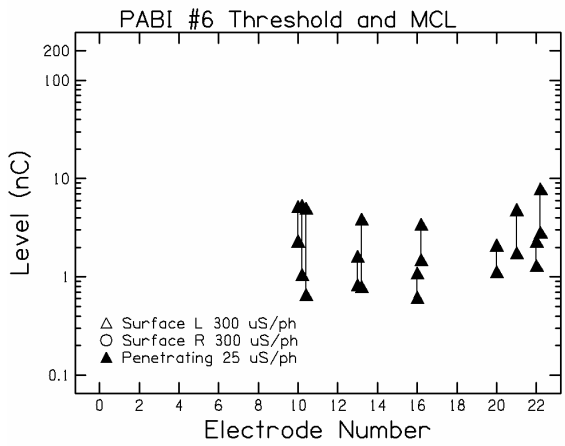

Figure 2

Figures 1-5 present threshold and dynamic range measures from PABI patients 4, 6, 7, 8, and 9, respectively. Each cluster of data points represent repeated measures over time, with the time interval between data points typically 3 months. Electrodes designated as "Surface L" (or "Surface R") are located along the left (right) side of the array as viewed face-on to the electrode contact surface and with the cable end pointing down. Each pair of two points connected by vertical lines represent the threshold and maximum comfortable loudness levels measured using the standard clinical method. Surface electrodes are shown as open symbols and penetrating electrodes are shown as filled symbols. In most cases the repeated measures show good stability over time. PABI#4 has excellent low threshold levels on most surface electrodes (less than 5 nC) and no responses on any of her penetrating electrodes.

PABI#6 received no auditory sensation on any surface electrodes but initially received auditory sensations on most of his penetrating electrodes. Some facial stimulation was reported on some penetrating electrodes that developed into strong adverse pain responses on most of the penetrating electrodes. At the most recent testing this patient was only able to use a single

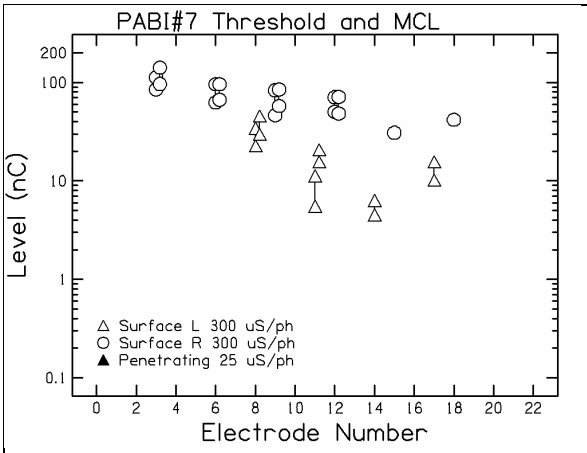

Figure 3

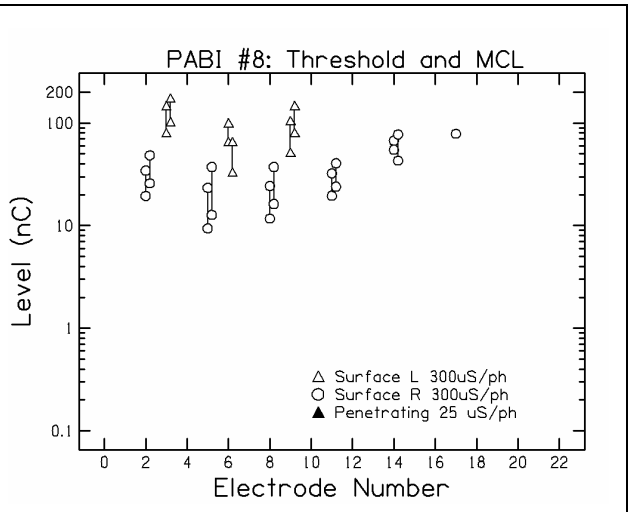

Figure 4

penetrating electrode - all other penetrating electrodes caused painful sensation in the ipsilateral face. These sensations are likely due to activation of the spinal root of the trigeminal nucleus (see last progress report for detailed descriptions of the testing and diagnosis of this problem). Three of the penetrating electrodes had thresholds of less than 1 nC, but electrodes 13 and 16 subsequently produced facial pain and so were not useful in a sound processor.

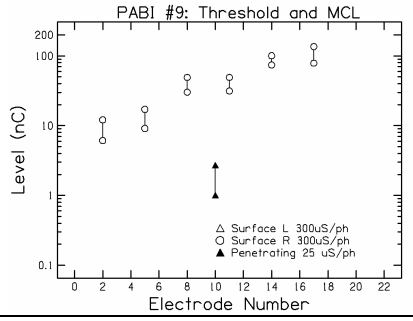

Figure 5

PABI#7 received no auditory sensations on his penetrating electrodes and moderate threshold levels on his surface electrodes. This patient also received strong facial pain on two of the penetrating electrodes. Surface electrodes 11, 14, and 17 had threshold levels below 10 nC, but electrodes 14 and 17 also produced nonauditory side effects (NASE) that made them unsuitable for use in a speech processor. Electrodes on one side of the array (3, 6,. 9, 12, etc) had higher threshold levels that electrodes on the other side (8, 11, 14, 17) indicating that the electrode has one edge closer to stimulable tissue than the other. This is a common pattern of results for PABI surface electrodes and regular ABI devices.

PABI#8 was implanted on March 30, 2006 and received her initial activation on October 3, 2006 (the delay in initial activation was due to the unexpected non-auditory sensations experienced by PABI#6 and #7 and the initial activation of PABI#8 was postponed until we resolved the probable cause of those NASE). She received no auditory sensations from her penetrating electrodes and a moderate pattern of thresholds on her surface electrodes. She received nonauditory sensations on several penetrating electrodes (sharp sensation in throat, sharp sensation in tongue, and tingling in the ipsilateral face and ear) but no useful auditory sensations. It is not clear if the NASE result from activation of the spinal root of the trigeminal nucleus, as was observed in PABI 6&7. The nonauditory sensations were milder in PABI8 than in PABI 6&7, and they occurred at high stimulation levels, while the NASE in PABI 6&7 occurred at stimulation levels below 1 nC.

PABI 9 was implanted on September 12, 2006 and received her initial activation on November 14, 2006. The surgical/anatomical team felt that the placement of this penetrating electrode array was ‘ideal”; the anatomical landmarks were clearly identifiable and the electrode was placed at the junction of the taenia and VIII nerve stump. Excellent electrophysiological responses identified by the electrophysiologist as due to activation of

auditory pathways were obtained from stimulation of the penetrating electrode array intraoperatively. Unfortunately, she received sound perception on only one penetrating electrode and on several surface electrodes along one side of the surface array. She received mild sensations in the ipsilateral eye on many penetrating and surface electrodes. The location of the NASE and the stimulation levels at which they occurred suggest that they were due to activation of the flocculus of the cerebellum and/or inferior cerebellar peduncle (ICP) rather than the spinal root of the trigeminal nerve. She perceived a high pitch sensation on the one penetrating electrode at a low stimulation level of less than 1 nC. Her surface electrode threshold levels increased with the electrode numbers, indicating that the cable end of the array was in the best position over the nucleus.

In summary, we now have 9 PABI patients implanted and activated. Five of the nine receive usable auditory sensations on at least one penetrating electrode, although three of those five receive hearing on only one penetrating electrode. Four patients receive hearing on surface electrodes but no hearing from the penetrating electrodes. In one of these patients (#4) x-ray evidence confirms movement of the penetrating electrode array following surgery.

Fig 6: ABI Speech Recognition over Time

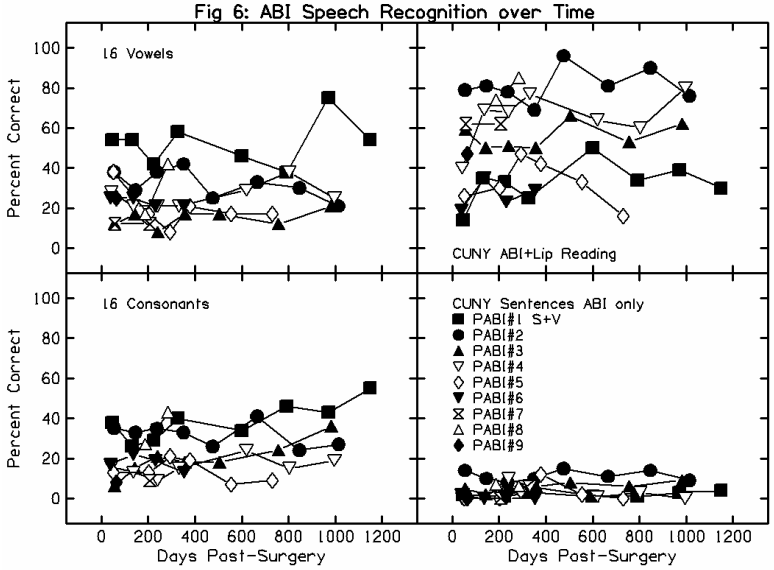

Speech Recognition

Figure 6 shows results from selected speech recognition measures over time for all PABI patients. Filled symbols present results from PABI patients who use penetrating electrodes in their speech processor maps and open symbols present results from patients who cannot use penetrating electrodes in their maps. The two left panels show results from vowel (upper) and consonant (lower) phoneme recognition tests. Chance performance is 12.5% correct on the vowel test and 6.25% correct for the consonant test. Due to her low overall level of performance PABI#1 was tested on these phonemes using both the sound from the PABI device and lipreading (S+V). The right panels show recognition of simple sentences (CUNY) either using only the sound from the PABI (lower panel) or in combination with lip-reading (upper panel). Although there are a small number of PABI patients, these preliminary data show no clear evidence of performance improvements compared to standard surface electrode ABI devices.

Figure 7: Threshold vs Pulse Rate

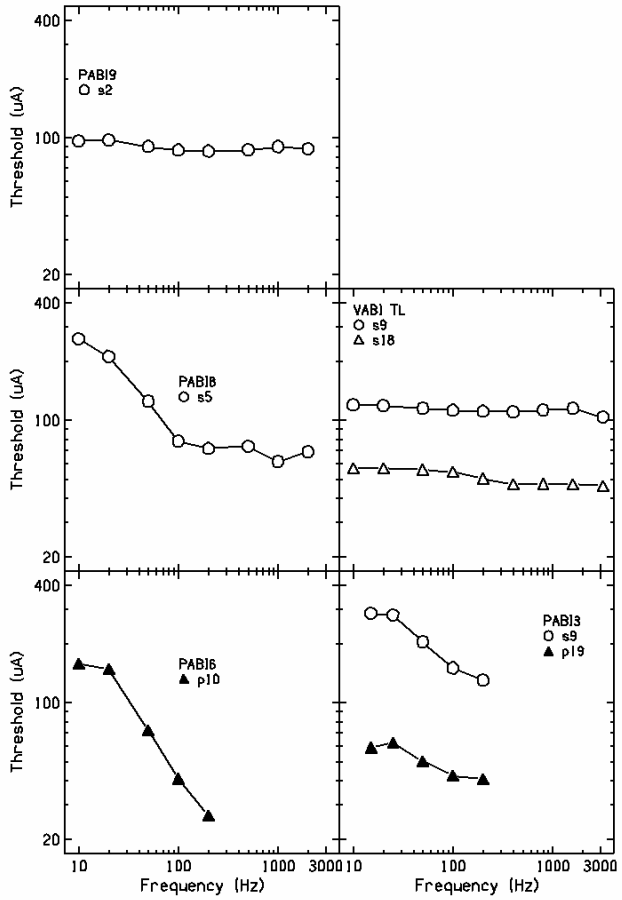

Threshold as a Function of Pulse Rate Thresholds were measured as a function of pulse rate for PABI 6, 8 and 9 during this reporting period and the results are presented in Figure 7 in the left three panels. Similar data from one non-NF2 ABI patient (VABI TL) and PABI#3 are repeated from the last progress report for comparison in the right two panels. Open symbols present results from surface electrodes and filled symbols present results from penetrating electrodes. There appears to be considerable difference across patients in this measure. Three of the four PABI patients (3, 6, and 8) show a significant integration across pulses for pulse rates between 20 pps and 100-200 pps. As the pulse rate increases threshold levels drop significantly on both surface and penetrating electrodes. In contrast, PABI#9 and non-NF2 ABI patient TL showed little change in threshold levels across stimulation rates. This flat pattern is more typical of results in cochlear implants. The falling pattern of thresholds suggests integration across stimulation pulses with a time constant of 50-100 ms. Both penetrating electrodes tested showed this falling threshold pattern indicating integration, but it is not clear if there is a difference between surface and penetrating electrodes. In the only patient in whom we measured thresholds on both surface and penetrating electrodes (PABI #3, lower right panel) both curves showed a similar pattern of falling thresholds.

Threshold as a Function of Pulse Phase Duration

Figure 8 presents measures of threshold as a function of pulse phase duration. Stimulation rates were low (10-20 Hz) in an attempt to avoid cross-pulse integration. However, in light of the results shown in Figure 7, 20 Hz might still indicate some cross-pulse integration. The left three panels show results from PABI patients 6, 8, and 9 obtained during this quarter while the right three panels show results from PABI patients 2 and 3 from the previous quarter. The lower right panels presents results from seven non-NF2 ABI patients with surface electrodes. Note that most of the curves from surface and penetrating electrodes show approximately linear relations between threshold and pulse phase duration. The slope of the line shows the trade-off between pulse phase amplitude and phase duration. Equal charge at threshold would result in flat horizontal lines, i.e. amplitude and duration trade equally. However the slope is approximately 0.5 for most curves, indicating that the pulse amplitude trades off with the square root of pulse phase duration to achieve equal sensation magnitude. Most results show no horizontal segment, which implies that the lowest amount of charge is needed at the shorted pulse phase durations. However, PABI 3 and 6 do show a flat portion of the function for phase durations below 100 us. Short pulses for these two PABI patients do show an equal trade-off between pulse amplitude and phase duration, resulting in

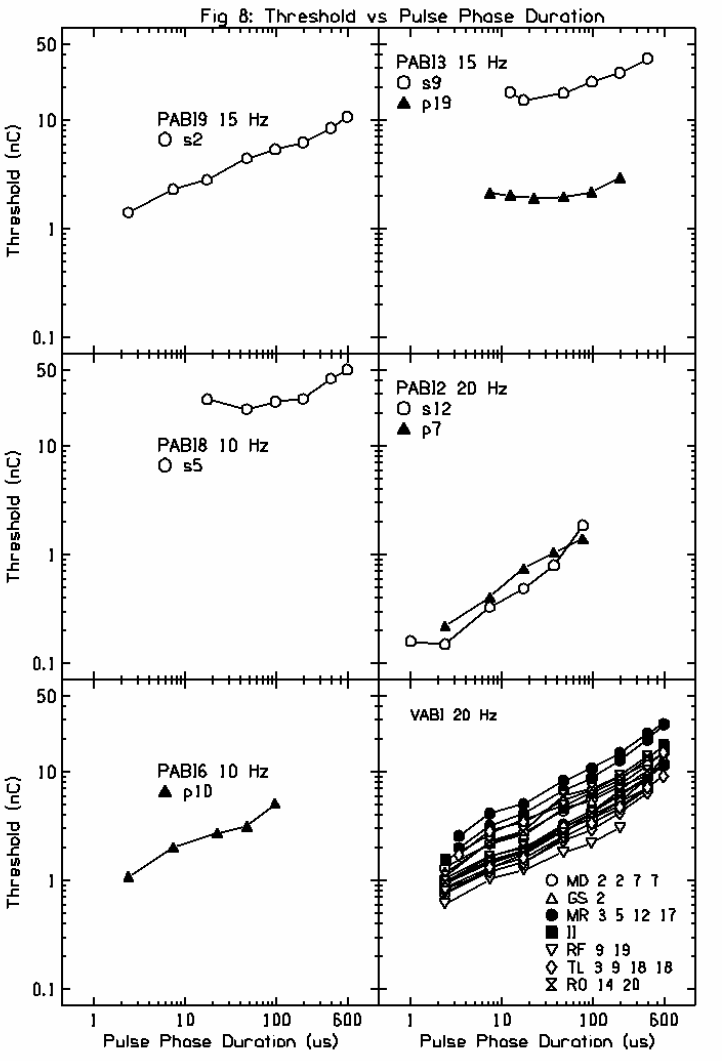

a constant chare for threshold. PABI#3 also showed equal charge at threshold for short pulses on his penetrating electrode. However PABI#6 showed no such constant charge portion on his threshold function for a penetrating electrode. Note that PABI #3 and #8 also showed significant integration of pulses as a function of pulse rate in Figure 7. But PABI #6, who had significant integration of pulses as a function of rate, did not show constant charge at threshold as a function of pulse duration.

Gap Detection

Gap detection is an indication of the ability to resolve silent intervals in an ongoing sound. Measures collected from PABI #8 and #9 during this quarter are shown in Figure 9. Gap detection is plotted as a function of the loudness of the stimulus, judged by the subject on a numerical scale from 0 to 10. Comfortable loudness is usually assigned a number of 5-6 on this scale. Average gap detection thresholds +/- 1 standard deviation are shown as the hatched area for 40 cochlear implant and ABI listeners; gap thresholds are typically longer when the stimulus is soft and shorten when the stimulus is louder. PABI #9 showed gap detection thresholds in the normal range for surface electrode s2 but abnormally long gap thresholds (50-100 ms) for penetrating electrode p10. It is unusual in our experience to see such large differences in gap detection across electrodes. Although there is variation in gap detection across listeners we have generally seen similar gap thresholds across electrodes for an individual listener. PABI #8 showed higher than normal gap thresholds for surface electrode s5. She was only able to detect gap thresholds of 50 ms even when the stimulus was quite loud. For soft sounds she was only able to detect a gap of 200 ms, which a typical syllabic duration.

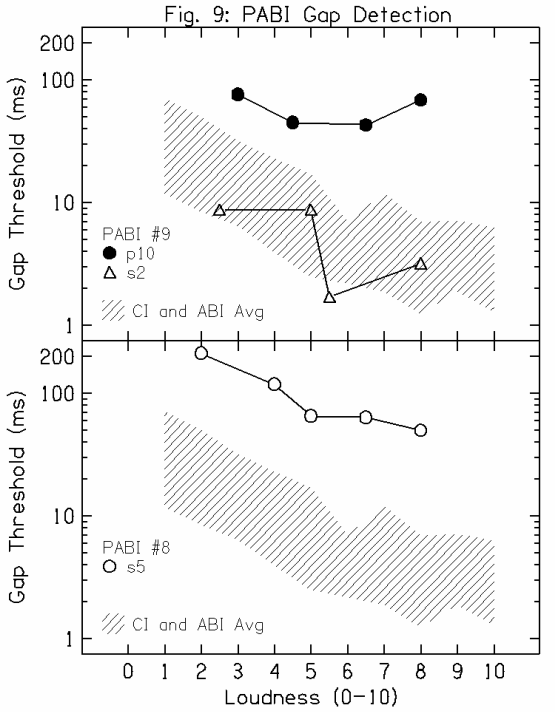

Summary

Measures on PABI patients in this quarter showed a mixed picture of results. In the two new PABI patients tested in this quarter only one had useful auditory sensations on the penetrating electrodes, and she only had one usable penetrating electrode. In total, four of 9 PABI patients receive no auditory sensations on the penetrating electrodes and three of the other five only receive auditory sensations on one penetrating electrode. We continue to observe speech recognition performance in PABI patients that is similar to that of surface ABI patients. We see little improvement in speech recognition performance out to three years. Psychophysical measures show some PABI patients to perform significantly worse than surface ABI and CI patients, while most are similar to ABI and CI listeners. The only psychophysical measure that is different in some PABI patients is the integration of pulses as a function of pulse rate, resulting in lower thresholds as rate increases. The cause of this difference is not clear at this time and this difference does not appear to be related to speech recognition performance.

Presentations

Shannon, RV (2006). "Assembling the bits - or not: Implications of auditory implants for speech recognition", Pisonifest, Bloomington, IN, Oct 20.

Shannon, RV (2006). "Speech recognition and psychophysical results from electrical stimulation of the human cochlea, cochlear nucleus and inferior colliculus", Acoustical Society of America, LA Chapter, Nov 14.

Shannon, RV (2006). "Electrical stimulation of the Human Cochlea, Brainstem and Midbrain: Implications for speech pattern Recognition", Boston University, Department of Biomedical Engineering, Nov 16.

Shannon, RV (2006). "Restoration of Hearing from Electrical Stimulation of the Human Cochlea, Brainstem and Midbrain", Polytrauma Conference, Dartmouth University, Dec 3-4.